Applied Mathematical Modelling 53 (2018) 709–721

Contents lists available at ScienceDirect

Applied Mathematical Modelling

journal homepage: www.elsevier.com/locate/apm

Group-based concurrent transmissions for spatial efficiency in IEEE 802.15.7 visible light communications☆

Jung-Hyok Kwon, Sol-Bee Lee, Eui-Jik Kim*

Department of Convergence Software, Hallym University, 1 Hallymdaehak-gil, Chuncheon-si, Gangwon-do 24252, South Korea

ARTICLE INFO

Article history:
Received 23 August 2016
Revised 23 August 2017
Accepted 29 August 2017
Available online 9 September 2017

Keywords:
Concurrent transmission
Device grouping
IEEE 802.15.7
Spatial efficiency
Visible light communication

ABSTRACT

This paper presents a group-based concurrent transmission (GCT) scheme for visible light communications (VLCs), which aims to improve the spatial efficiency of IEEE 802.15.7-based VLC personal area networks (VPANs). To this end, the GCT combines the VLC devices that interfere with each other into a group taking into account the directionality of the light sources, and thus allows the concurrent transmissions of device groups. Then, it differentiates the BE value of each device group according to the number of VLC devices in the group, to prevent unnecessary backoff delay and collision. The GCT has two main operations: (1) VLC device grouping and (2) concurrent transmission scheduling. In the former, each device conducts neighbor discovery to create VLC device table (VDT) entries, through which the central controller builds groups considering the interference between neighbors. In the latter, the BE decision procedure is performed, in which the central controller allocates the different BE value to each group in accordance with the number of devices belonging to the group. To evaluate the performance of GCT, we developed the analytical model using the discrete-time Markov chain. The numerical results show that the GCT achieves a better network performance than the IEEE 802.15.7 standard.

1. Introduction

Visible light communication (VLC) refers to short-range optical wireless communication where the devices transmit data via light sources, such as light-emitting diodes (LEDs) and laser diodes (LDs). The VLC that uses the unlicensed visible light spectrum (380–780 nm) is being considered as an emerging technology to replace radio frequency (RF)-based communication, which suffers from a lack of available radio frequency. The VLC has many advantages including high directionality, wide bandwidth, and license-free communication, thus it can be utilized in various application domains such as hospitals and airplanes where the communication is very restricted and does not interfere with existing legacy RF systems. In addition, the VLC can reuse existing light infrastructures for communication, such as indoor light, signboards, vehicles, and television [1–6].

In 2011, IEEE 802.15 task group 7 (TG 7) specified the IEEE 802.15.7 standard for VLC, which provides detailed physical (PHY) and medium access control (MAC) layers specification for short-range optical wireless communications using visible light [7]. The IEEE 802.15.7 supports three network topologies: peer-to-peer, star, and broadcast and defines four types of channel access mechanisms: slotted random access with or without carrier sense multiple access/collision avoidance

☆ "This article belongs to the Special Issue: IMETI-2015 International Multi-Conference on Engineering and Technology Innovation 2015".

* Corresponding author.
E-mail address: ejkim32@hallym.ac.kr (E.-J. Kim).

http://dx.doi.org/10.1016/j.apm.2017.08.033
0307-904X/

(CSMA/CA) for beacon-enabled VLC personal area networks (VPANs), and unslotted random access with or without CSMA/CA for non-beacon-enabled VPANs. In the slotted random access mechanism, a VPAN coordinator periodically transmits the beacon frame to align the slots. In beacon-enabled mode, the VPAN coordinator divides its channel time into superframes, which are comprised of active and optional inactive durations. In the active duration, the coordinator communicates with devices within the VPAN, which enter low-power mode (i.e., sleep mode) during the inactive duration. The active duration consists of a contention access period (CAP) and a contention-free period (CFP). In the CAP, the devices in VPAN contend with each other to access the channel based on the CSMA/CA. The CFP uses the guaranteed time slot (GTS) reserved by the VPAN coordinator to ensure the transmission of dedicated devices.

The CSMA/CA mechanism of IEEE 802.15.7 MAC standard overlooked the directionality of the light source. The directionality is an important and advantageous property of VLC and increases concurrent transmissions with neighboring devices, which can significantly improve network performance of VPAN. Nevertheless, in the CSMA/CA of IEEE 802.15.7 standard, both the backoff and clear channel assessment (CCA) procedures are designed under the assumption that the light source has an omnidirectional feature, thus the current standard cannot support concurrent transmissions of the VLC devices and degrades the network performance of VPAN in terms of the spatial efficiency. In particular, regarding the backoff procedure, the IEEE 802.15.7 standard uses a fixed value of backoff exponent (BE) regardless of the density and collision of the VLC devices, which causes unnecessary backoff delay in the area where the devices are sparsely distributed, and degrades the network performance due to the collisions in the area where the devices are concentrated**.**

Considering that most VLC applications use multiple devices in a limited space, it is essential to control the medium access, operation mode, and device association [8]. Therefore, in addition to the IEEE 802.15.7 standard, various link-layer technologies for VLC have been studied to improve network performance, such as throughput, delay, and energy consumption [9,10]. In [11,12], multiple-input multiple-output (MIMO) technology is considered for VLC to increase the channel capacity. Specifically, Mmbaga et al. proposed the non-line of sight (NLOS) model to identify the transmitter in an indoor VLC MIMO channel [11]. In particular, they considered the indoor environment to use the reflected light from the ceiling and wall for modeling. Hong et al. presented the MIMO indoor VLC system using the block diagonalization precoding algorithm for multi-users [12]. Their system was designed to reduce the power consumption and the complexity of user devices. The adaptive MAC protocol was also considered a challenging issue [13]. Wang et al. proposed the self-adaptive minimum contention window-based full-duplex MAC (SACW) protocol for VLC [14]. The SACW adopted different contention window sizes to reduce the channel access delay. The VLC often uses optical *attocell*, which is a similar concept to *femtocell* in RF communication. Chen et al. proposed fractional frequency reuse (FFR) based on direct-current optical orthogonal frequency division multiplexing (DCO–OFDM) for optical *attocell* networks to mitigate interference [15]. Several studies focus on the coexistence of technologies for VLC. Wang et al. proposed hybrid dynamic load balancing (LB), which selectively provides light fidelity (Li-Fi) or RF wireless fidelity (Wi-Fi) capabilities for users [16]. The LB provides Li-Fi capabilities to stationary users and Wi-Fi capabilities to moving users. However, to the best of our knowledge, no current study focuses on the concurrent transmission issue for spatial efficiency for allowing simultaneous communications in a limited service area.

In this paper, we propose a group-based concurrent transmission (GCT) scheme for VLCs, which aims to improve the spatial efficiency of IEEE 802.15.7-based VPANs. To this end, the GCT combines the VLC devices that interfere with each other into a group taking into account the directionality of the light sources, and thus allows the concurrent transmissions of device groups. Then, it differentiates the BE value of each device group according to the number of VLC devices in the group, to prevent unnecessary backoff delay and collision. The GCT has two main operations: (1) VLC device grouping and (2) concurrent transmission scheduling. In the former, each device conducts neighbor discovery to create VLC device table (VDT) entries, through which the central controller (i.e., the VPAN coordinator) builds groups considering the interference between neighbors. In the latter, the BE decision procedure is performed, in which the central controller allocates the different BE value to each group in accordance with the number of devices belonging to the group. To evaluate the performance of GCT, we developed an analytical model using a discrete-time Markov chain, through which we derived various probabilities for a device in the group, such as transmission probability, collision probability, and the probability that the channel is idle [17–21]. Then, we evaluated the normalized throughput and average delay for a single group and the aggregate throughput and average delay for the entire groups. We compared the performance of GCT with that of the IEEE 802.15.7 standard. The numerical results show that the GCT has better performance in terms of spatial efficiency compared with the IEEE 802.15.7 standard.

The rest of this paper is organized as follows. In Section 2, we present the system model of GCT. The design of GCT is described in detail in Section 3. The numerical analysis and performance analysis are provided in Sections 4 and 5, respectively. Section 6 provides the numerical results, which verify the effectiveness of GCT. Finally, Section 7 concludes this paper.

2. System model

Fig. 1 shows the system architecture of GCT, which consists of multiple VLC devices and a single central controller. Each device has an LED as a transmitter and a photodiode as a receiver, which communicate with each other in a half-duplex. These VLC devices emit their narrow fan shape of light toward a certain direction, and the line-of-sight (LOS) feature should be guaranteed for their communications [22,23]. In GCT, all the VLC devices are assumed to use the same degrees of the field of view (FOV) to maintain the same communication coverage. It is further assumed that the VLC devices are static

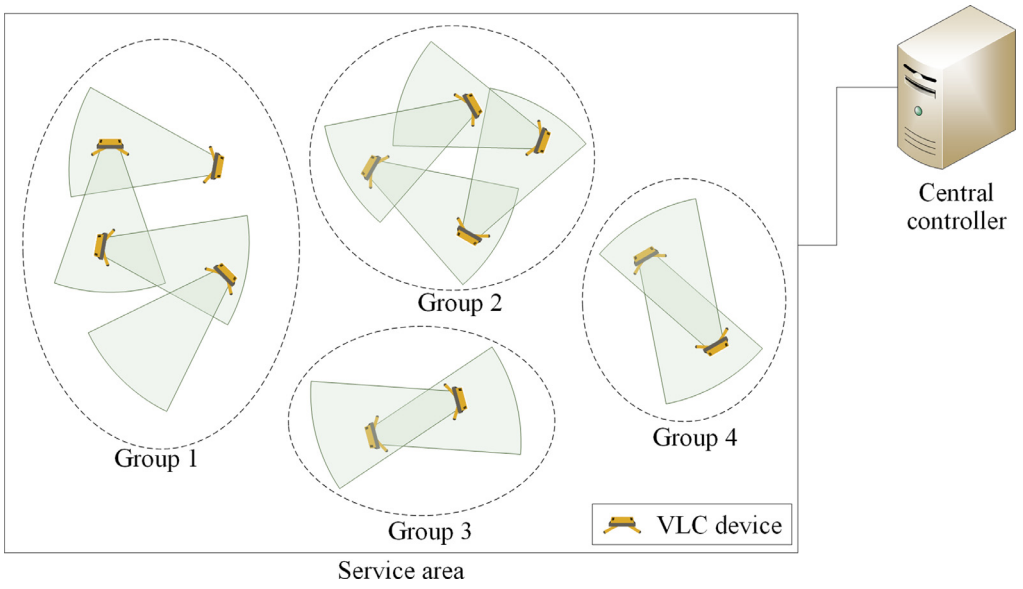

Fig. 1. System architecture of GCT.

or semi-static and connected to the central controller via either wireless or wired link. The central controller periodically communicates with the devices for various operations, such as synchronization, MAC scheduling, and group management. In our work, the central controller generates the VLC device groups for allowing the concurrent transmission within the adjacent area considering the interference range of the devices.

As shown in the figure, we consider the peer-to-peer topology of VLC, where one of a pair of devices serves as the master of the VLC link, and the devices in VPAN operate based on the superframe structure, including both active and inactive periods that are scheduled by the central controller. On the superframe, the devices use the slotted random access mechanism with CSMA/CA and beacon-enabled mode specified in the IEEE 802.15.7 standard [7].

3. Group-based concurrent transmissions

The GCT is designed to improve the spatial efficiency of IEEE 802.15.7-based VPAN. To this end, the GCT provides two main operations: (1) VLC device grouping and (2) concurrent transmission scheduling. In the following subsections, we describe the design of GCT scheme in detail.

3.1. VLC device grouping

In the operation of VLC device grouping, the central controller binds all the devices within the service area into several groups. To this end, the controller maintains the VDT table, whose entries include the IDs of interfering neighbors**.** At the beginning of the beacon interval, each device runs a neighbor discovery procedure to create the VDT table, for which it periodically broadcasts a hello message with its own device ID. Upon receiving the hello message, the device first checks the device ID in the received message and caches it as the interfering neighbor. Once the neighbor discovery is completed, the devices deliver the gathered information to the central controller, which updates its own VDT table entries and starts to build the groups using the VDT.

Algorithm 1 describes the operation of VLC device grouping in detail. In the algorithm, a set of VLC devices within a service area is represented by matrix **D**, as in Eq. (1),

$$\mathbf{D} = \left[d_{(1)}, d_{(2)}, d_{(3)}, \ldots, d_{(i)}, \ldots, d_{(n_d)}\right], 1 \le i \le n_d \tag{1}$$

where n_d is the total number of devices within the service area and $d_{(i)}$ is the device ID of the ith device. First, each device constructs its own temporary group including the device itself and its neighbors, namely the neighbor matrix, which can be represented using the matrix $\mathbf{N}_{(i)}$, as in Eq. (2) (i.e., lines 2–4).

$$\mathbf{N}_{(i)} = \left[d_{(i,0)}, d_{(i,1)}, d_{(i,2)}, \ldots, d_{(i,j)}\right], 0 \le j \le n_d - 1 \tag{2}$$

where $d_{(i,0)}$ refers to its own device ID, and other elements are the device IDs of the neighbors. Note that, in our work, a set of devices interfering with each other can construct one group. Thus, to create the group, each device uses the matrix $\mathbf{N}_{(i)}$. Each device compares all the elements of its own $\mathbf{N}_{(i)}$ with those of $\mathbf{N}_{(k)}$ of other devices, in a pairwise manner (i.e., lines 15–21). If there exists any intersected element in matrix $\mathbf{N}_{(i)}$ (i.e., $\mathbf{N}_{(i)} \cap \mathbf{N}_{(k)} \neq \varphi$), the compared matrixes can be merged

Algorithm 1. VLC device grouping.

```
1: INITIALIZE i to 1, a to 1
2: FOR each device, i, i ∈ [1, n_d] //n_d is the number of devices
3:   N_(i) = [d_(i,0), d_(i,1), d_(i,2), ..., d_(i,j)] // Construct a neighbor matrix for each device.
4: ENDFOR
5: FOR each device, i, i ∈ [1, n_d]
6:   IF i ≥ 2
7:     FOR j, j ∈ [1, i − 1] // Check the intersected element.
8:       IF N_(i) ∩ N_(j) ≠ φ
9:         CONTINUE
10:      ENDIF
11:    ENDFOR
14:  ENDIF
15:  FOR each device, k, k ∈ [1, n_d]
16:    IF N_(i) ∩ N_(k) ≠ φ
17:      N_(i) ← N_(i) ∪ N_(k)
18:    ELSE
19:      N_(i) ← N_(i)
20:    ENDIF
21:  ENDFOR
22:  G_(a) ← N_(i)
23:  a ← a + 1
24: ENDFOR
```

into one group, which is a union set, $\mathbf{N}_{(i)} \cup \mathbf{N}_{(k)}$. If not, they cannot be merged; each neighbor matrix itself is created to one group. As a result, a set of devices belonging to the created group can be represented by the matrix $\mathbf{G}_{(a)}$, as in Eq. (3),

$$\mathbf{G}_{(a)} = \left[g_{(a,1)}, g_{(a,2)}, g_{(a,3)}, \ldots, g_{(a,l_a)}\right], 1 \le a \le n_d, 1 \le l_a \le n_d \tag{3}$$

where a is the group ID, l_a is the number of devices within a group a, and $g_{(a,j)}$ is the device ID of the l_ath device within group a.

Algorithm 1 is a process of checking whether or not the transmission area (i.e., FOV) of each VLC device is overlapped and forming a device group if not overlapped. Neighboring VLC devices with overlapping transmission areas become interfering neighbors. Each VLC device collects the IDs of the interfering neighbors by exchanging hello messages with the neighbors in the neighbor discovery procedure. The controller maintains the IDs of the interfering neighbors as VDT table entries, through which it performs the operation of device grouping.

3.2. Concurrent transmission scheduling

The devices belonging to the different groups do not interfere with each other; thus, they can transmit data simultaneously, while the devices within the same group have to contend with each other to grab the channel using the CSMA/CA. In other words, in the latter case, only the device that wins the contention can transmit data at a certain time. The IEEE 802.15.7 standard uses a fixed BE, which may cause long backoff delay and frequent collisions. Note that BE is the backoff exponent which is closely related to the number of backoff periods. The device waits for a random number of backoff periods in the range of $[0, 2^{BE} - 1]$ before attempting to assess the channel [17,21]. To address this problem, the GCT applies a different BE value to each group depending on the number of devices within a group, whose value needs to be decided to improve the spatial efficiency of the whole system. For this, the GCT performs the concurrent transmission scheduling procedure through the BE decision, which adjusts the BE value in accordance with the number of devices within a group. The central controller classifies each group into multiple classes, each of which has a specific class range that can be given as Eq. (4).

$$\begin{cases} \text{Range of class } 1 = \left[1, \dfrac{1}{n_c} \times n_d\right), n_c \le n_d \\ \text{Range of class } 2 = \left[\dfrac{1}{n_c} \times n_d, \dfrac{2}{n_c} \times n_d\right), n_c \le n_d \\ \text{Range of class } 3 = \left[\dfrac{2}{n_c} \times n_d, \dfrac{3}{n_c} \times n_d\right), n_c \le n_d \\ \vdots \\ \text{Range of class } n_c = \left[\dfrac{n_c - 1}{n_c} \times n_d, n_d\right], n_c \le n_d \end{cases} \tag{4}$$

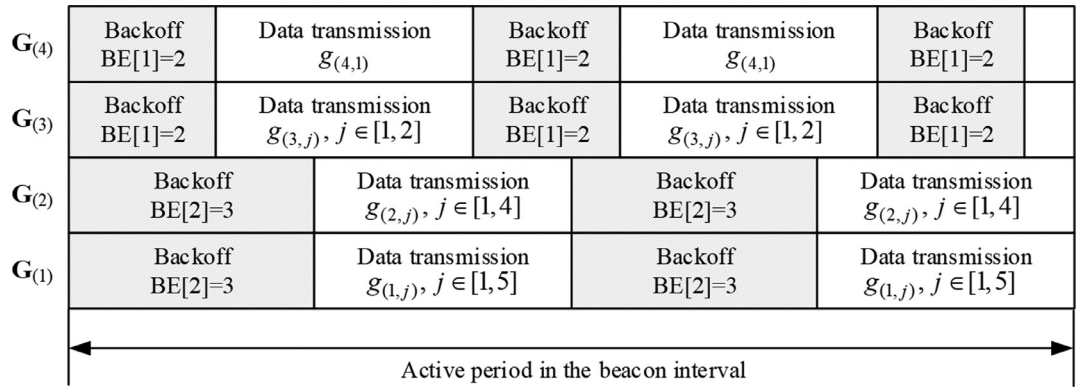

Fig. 2. Example of concurrent transmission scheduling.

where n_c is the number of classes that is defined in advance by the central controller. The central controller assigns a different class ID (i.e., q_a) to each group a based on the number of devices within each group, as in Eq. (5).

$$\begin{cases} q_a = 1, l_a \in \left[1, \frac{1}{n_c} \times n_d\right), n_c \le n_d \\ q_a = 2, l_a \in \left[\frac{1}{n_c} \times n_d, \frac{2}{n_c} \times n_d\right), n_c \le n_d \\ q_a = 3, l_a \in \left[\frac{2}{n_c} \times n_d, \frac{3}{n_c} \times n_d\right), n_c \le n_d \\ \vdots \\ q_a = n_c, l_a \in \left[\frac{n_c - 1}{n_c} \times n_d, n_d\right], n_c \le n_d \end{cases} \tag{5}$$

where l_a is the number of devices within group a. For example, if l_a is in the range of $[1, \frac{1}{n_c} \times n_d)$, q_a is set to 1. The central controller selects a different BE for each group according to its q_a. The value of BE for q_a (i.e., BE$[q_a]$) can be given as shown in Eq. (6).

$$\mathrm{BE}[q_a] = \begin{cases} w + q_a, w + q_a < \mathrm{macMaxBE} \\ \mathrm{macMaxBE}, w + q_a \ge \mathrm{macMaxBE} \end{cases} \tag{6}$$

where w is the weight factor of BE$[q_a]$ and macMaxBE is the maximum value for BE$[q_a]$ defined in the IEEE 802.15.7 standard [7]. The GCT uses the IEEE 802.15.7 standard as the baseline MAC scheme, which employs a binary exponential backoff (BEB) algorithm. Thus, the VLC device attempts to avoid collisions between the neighbors by generating random backoff periods in the range of $[0, 2^{\mathrm{BE}[q_a]} - 1]$. In this case, the number of backoff periods should be greater than the number of devices in the group, and therefore the central controller should select the value of w in consideration of the values of n_d and n_c. In other words, 2^{w+n_c} is greater than or equal to the value of n_d, thus to minimize the backoff delay, the value of w is given by Eq. (7)

$$w = |\log_2(n_d) - n_c + 1|, \tag{7}$$

Fig. 2 illustrates an operational example of concurrent transmission scheduling. In the figure, the number of classes (i.e., n_c) is 3, the total number of devices (i.e., n_d) is 12, and there exist 4 VLC device groups (i.e., $\mathbf{G}_{(1)}$, $\mathbf{G}_{(2)}$, $\mathbf{G}_{(3)}$, $\mathbf{G}_{(4)}$). Using Eq. (7), the value of w is calculated as 1, and each group can be represented as follows: $\mathbf{G}_{(1)} = [g_{(1,1)}, g_{(1,2)}, g_{(1,3)}, g_{(1,4)}, g_{(1,5)}]$, $\mathbf{G}_{(2)} = [g_{(2,1)}, g_{(2,2)}, g_{(2,3)}, g_{(2,4)}]$, $\mathbf{G}_{(3)} = [g_{(3,1)}, g_{(3,2)}]$, $\mathbf{G}_{(4)} = [g_{(4,1)}]$. Through the BE decision, we obtain the BE$[q]$ value of each group. As a result, $\mathbf{G}_{(1)}$ has BE[2] = 3, $\mathbf{G}_{(2)}$ has BE[2] = 3, $\mathbf{G}_{(3)}$ has BE[1] = 2, and $\mathbf{G}_{(4)}$ has BE[1] = 2.

Upon completing the BE decision, the central controller assigns the selected BE$[q_a]$ to all groups. When the data transmission period of the superframe starts, the devices communicate with each other with the selected BE$[q_a]$. Algorithm 2 describes the operation of transmission scheduling. Each device executes the algorithm using BE$[q_a]$ assigned from the central controller in a distributed manner. First, the three variables (i.e., n, c, and b) are initialized, where n is the number of backoff stages (NB) referring to the number of transmission attempts, c is the value of the clear channel assessment (CCA) counter that defines the number of times the channel status (i.e., idle or busy) will be assessed, and b is the value of the backoff counter that denotes the number of backoff periods the device should wait before assessing the channel status. n and c are initialized to 0 and 1, respectively, and b is initialized to an integer value randomly selected between 0 and $2^{\mathrm{BE}[q_a]} - 1$. The device can try to transmit up to $m+1$ times until its packet transmission is successful, where m is the maximum value of NB. In each transmission attempt, the device waits for b backoff periods and then performs the CCA procedure to check whether the channel is idle. If the channel is idle, the device transmits the packet and, if the transmission is successful,

Algorithm 2. Transmission scheduling.

```
1: INITIALIZE n to 0, c to 1, b to random(0, 2^BE[q_a] − 1)
2: FOR each backoff stage, n, n ∈ [0, m]
3:   IF b > 0
4:     b ← b − 1
5:   ELSE
6:     IF Channel status is idle // Clear channel assessment.
7:       c ← c − 1
8:       Transmission starts
9:       IF Collision occurs
10:          n ← n + 1, c ← c + 1, b ← random(0, min(2^BE[q_a]+n − 1, 2^macMaxBE − 1))
11:      ELSE // Transmission is successful.
12:          n ← 0, c ← c + 1, b ← random(0, 2^BE[q_a] − 1)
13:      ENDIF
14:    ELSE // Channel status is busy.
15:      n ← n + 1, b ← random(0, min(2^BE[q_a]+n − 1, 2^macMaxBE − 1))
16:    ENDIF
17:  ENDIF
18:  IF n = m + 1
19:    Channel access fails
20:  ENDIF
21: ENDFOR
```

initializes three variables (i.e., n, c, and b). On the other hand, if the channel is busy or the collision occurs, the both values of n and BE$[q_a]$ are increased by one to defer the transmission and to avoid the collisions. If n reaches $m+1$, the execution of algorithm for a current packet terminates with a channel access failure.

The execution of the GCT requires two types of control messages (i.e., information of interfering neighbors and BE decisions), which make up one transaction and their amount of data traffic is very small. Nonetheless, if the VLC devices are mobile, the GCT will be executed frequently and its overhead issue will be further exacerbated. However, since we assume a static or semi-static VLC device in this paper, the transactions of control messages for the GCT operation occur infrequently. Therefore, when considering a long period of network operation, the overhead problem is negligible.

4. Analytical model

To develop the analytical model of the GCT scheme, we consider the saturated condition, where each device always has a packet ready to be transmitted, and further assume the stationary devices and the ideal condition (i.e., no hidden terminal). Fig. 3 shows a state transition diagram for a device that runs the GCT. In the figure, we use three random variables for a given device in the group a. Let $n(q_a, t)$, $c(q_a, t)$, $b(q_a, t)$ be the stochastic processes that represent the NB, the CCA counter, and the backoff counter at time t, respectively. These processes $n(q_a, t)$, $c(q_a, t)$, and $b(q_a, t)$ constitute a multi-dimensional Markov process representing the state of the packet at the boundary of unit backoff period. As mentioned earlier, the devices belonging to group a have a common class ID q_a which is not changed, thus the processes $n(q_a, t)$, $c(q_a, t)$, and $b(q_a, t)$ can be briefly denoted as $n(t)$, $c(t)$, and $b(t)$, respectively. The state space of Markov process is denoted as

$$\begin{aligned}\Omega = \{&n(t), c(t), b(t) | 0 \le n(t) \le m+1, 0 \le c(t) \le 1, 0 \le b(t) \le W_i - 1,\\ &i = 0, \ldots, m, n(t), c(t), \text{and } b(t) \text{ are integers}\},\end{aligned} \tag{8}$$

where $m = \text{macMaxCSMABackoffs}$, $W_0 = 2^{\text{BE}[q_a]}$, and $W_i = 2^i W_0$.

In Fig. 3, the one-step transition probabilities are given as follows. Note that for the simplicity of notations, we use the transition probabilities $P(i, j, k-1|i, j, k)$ instead of $P(n(t+1)=i, c(t+1)=j, b(t+1)=k-1|n(t)=i, c(t)=j, b(t)=k)$.

$$P(i, 1, k-1|i, 1, k) = 1, \quad i \in [0, m], \quad k \in [1, W_i - 1], \tag{9}$$

$$P(i, 0, 0|i, 1, 0) = p_I, \quad i \in [0, m], \tag{10}$$

$$P(0, 1, k|i, 0, 0) = (1 - p_C)/W_0, \quad i \in [0, m], \quad k \in [0, W_0 - 1], \tag{11}$$

$$P(i, 1, k|i-1, 1, 0) = (1 - p_I)/W_i, \quad i \in [1, m], \quad k \in [0, W_i - 1], \tag{12}$$

$$P(i, 1, k|i-1, 0, 0) = p_C/W_i, \quad i \in [1, m], \quad k \in [0, W_i - 1], \tag{13}$$

$$P(m+1, 0, 0|m, 1, 0) = 1 - p_I, \tag{14}$$

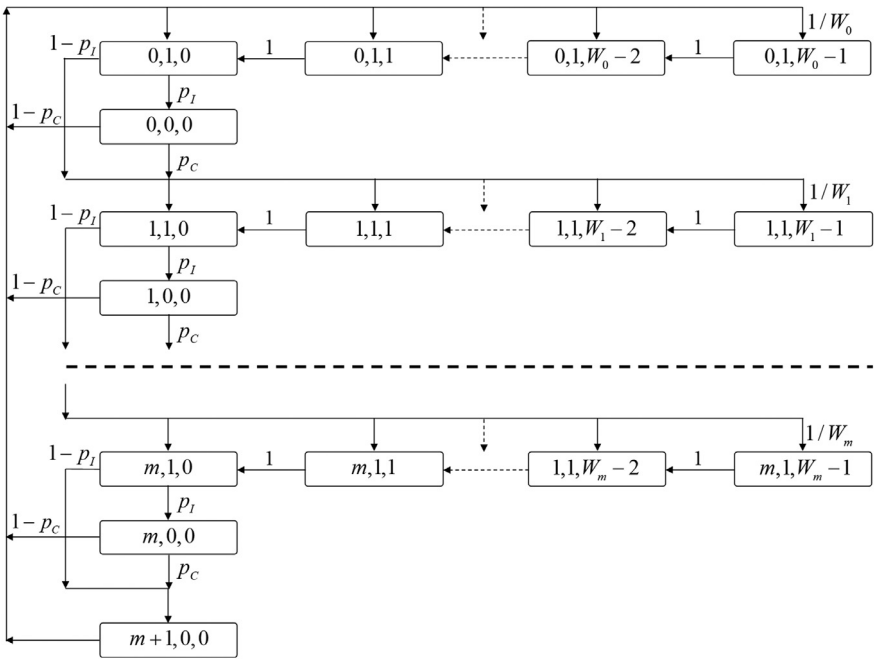

Fig. 3. Markov chain model.

$$P(m+1,0,0|m,0,0) = p_C, \tag{15}$$

$$P(0,1,k|m+1,0,0) = 1/W_0, \quad k \in [0, W_0 - 1], \tag{16}$$

where p_C is the collision probability and p_I is the probability that the channel is idle.

Eq. (9) represents the probability that the backoff counter decreases by one at the beginning of each time slot (i.e., unit backoff period). Eq. (10) is the probability that the CCA counter decreases from 1 to 0, after the channel is sensed idle in a time slot. Note that the IEEE 802.15.7 MAC includes only a single CCA procedure while in the IEEE 802.15.4 standard, the CCA is performed twice [21]. Eq. (11) is the probability that the transmission of a new packet starts at backoff stage 0 after the successful transmission. The probability of the successful transmission is $1-p_C$, and the initial value of the backoff counter is randomly selected in the range of $[0, W_0-1]$. Eqs. (12) and (13) are the probabilities that the device selects another random value of backoff counter in the next backoff stage, when the channel is sensed busy and the current transmission is unsuccessful, respectively, at the backoff stage $i-1$. In this case, the device uniformly selects the value of backoff counter in the range of $[0, W_i-1]$ at the bachoff stage i. Eqs. (14) and (15) are the probabilities that the current transmission fails at the maximum backoff stage (i.e., backoff stage m) when the channel is sensed busy and the collision occurs, respectively. Finally, Eq. (16) represents the probability that the current transmission fails and then the device starts to execute the algorithm again with a new packet at the backoff stage 0, thus its probability is $1/W_0$.

All states in the state space of Markov process are positive recurrence. Therefore, we can express the stationary probabilities $\{b_{i,j,k}\}$ of the discrete-time Markov chain as follows:

$$b_{i,j,k} = \lim_{t\to\infty} P\{n(t) = i, c(t) = j, b(t) = k\}, i \in [0,m], j \in [0,1], k \in [0, W_i - 1]. \tag{17}$$

The relations between stationary probabilities can be obtained as Eq. (18):

$$\begin{cases} b_{i,0,0} = b_{0,0,0}(p_I p_C + 1 - p_I)^i, \quad i \in [0,m], \\ b_{i,1,k} = b_{0,0,0}\dfrac{W_i - k}{W_i}\dfrac{(p_I p_C + 1 - p_I)^i}{p_I}, \quad i \in [1,m], \quad k \in [0, W_i - 1], \\ b_{0,1,k} = \dfrac{W_0 - k}{W_0}\left\{\sum_{i=0}^{m} b_{0,0,0}(p_I p_C + 1 - p_I)^i(1 - p_C) + b_{0,0,0}\dfrac{(p_I p_C + 1 - p_I)^{m+1}}{p_I}\right\}, \quad k \in [0, W_0 - 1], \\ b_{m+1,0,0} = b_{0,0,0}\dfrac{(p_I p_C + 1 - p_I)^{m+1}}{p_I}. \end{cases} \tag{18}$$

Then, it satisfies Eq. (19),

$$\begin{aligned}1 &= \sum_{i=0}^{m} b_{i,0,0} + \sum_{i=1}^{m}\sum_{k=0}^{W_i-1} b_{i,1,k} + \sum_{k=0}^{W_0-1} b_{0,1,k} + b_{m+1,0,0} \\ &= \sum_{i=0}^{m} b_{0,0,0}A^i + \sum_{i=1}^{m}\sum_{k=0}^{W_i-1} b_{0,0,0}\frac{W_i-k}{W_i}\frac{A^i}{p_I} + \sum_{k=0}^{W_0-1}\frac{W_0-k}{W_0}\left\{\sum_{i=0}^{m} b_{0,0,0}A^i(1-p_C) + b_{0,0,0}\frac{A^{m+1}}{p_I}\right\} + b_{0,0,0}\frac{A^{m+1}}{p_I} \\ &= b_{0,0,0}\left[\sum_{i=0}^{m} A^i + \sum_{i=1}^{m}\frac{A^i(W_i+1)}{2p_I} + \frac{W_0+1}{2}\left\{\sum_{i=0}^{m} A^i(1-p_C) + \frac{A^{m+1}}{p_I}\right\} + \frac{A^{m+1}}{p_I}\right]. \end{aligned} \tag{19}$$

In Eq. (19), $p_I p_C + 1 - p_I$ is replaced by A. Then, we obtain $b_{0,0,0}$ in Eq. (20),

$$b_{0,0,0} = \frac{2p_I}{\left[\frac{1-(2A)^{m+1}}{1-2A}W_0 + \frac{1-A^{m+1}}{1-A}\{p_I(W_0+3) - p_I p_C(W_0+1)\} + A^{m+1}(W_0+3) - (W_0+1)\right]}. \tag{20}$$

With the stationary probabilities, we derive the transmission probability τ that the device transmits a packet at the boundary of a backoff period as follows:

$$\begin{aligned}\tau &= \sum_{i=0}^{m} b_{i,0,0} = b_{0,0,0}\sum_{i=0}^{m} A^i = b_{0,0,0}\frac{1-A^{m+1}}{1-A} \\ &= \frac{2p_I}{\left[\frac{1-(2A)^{m+1}}{1-2A}\frac{1-A}{1-A^{m+1}}W_0 + p_I(W_0+3) - p_I p_C(W_0+1) + \frac{1-A}{1-A^{m+1}}\{A^{m+1}(W_0+3) - (W_0+1)\}\right]}, \end{aligned} \tag{21}$$

where τ depends on p_C and p_I. The collision occurs when at least one of the devices belonging to the group a, except for itself, transmits a packet. The collision occurs when at least one device among the devices in the group a other than itself transmits a packet. Moreover, the channel is sensed idle, if all the devices in the group a do not transmit packets. Therefore, p_C and p_I are obtained from Eqs. (22) and (23), respectively,

$$p_C = 1 - (1-\tau)^{l_a - 1} \tag{22}$$

$$p_I = (1-\tau)^{l_a}. \tag{23}$$

5. Performance analysis

Let S_a be the normalized throughput of group a, which is defined as the ratio of the average payload size transmitted from the devices belonging to the group a to the average length of slot time, as in Eq. (24) [24],

$$S_a = \frac{E(\text{payload transmitted from group } a \text{ in a slot time})}{E(\text{length of a slot time for group } a)}. \tag{24}$$

To derive S_a, we define $P_{tr,a}$ and $P_{s,a}$, which are the probability that at least one device in the group a transmits a packet in a slot time and the probability that exactly one device in the group a transmits a packet in a slot time, respectively, as in Eqs. (25) and (26),

$$P_{tr,a} = 1 - (1-\tau)^{l_a} \tag{25}$$

$$P_{s,a} = \frac{l_a\tau(1-\tau)^{l_a-1}}{P_{tr,a}} = \frac{l_a\tau(1-\tau)^{l_a-1}}{1-(1-\tau)^{l_a}}. \tag{26}$$

In the group a, the probability that a successful transmission occurs in a slot time is $P_{tr,a}P_{s,a}$, thus the payload size successfully transmitted in a slot time is $P_{tr,a}P_{s,a}L$, where L is the payload size transmitted from the devices belonging to group a. Let σ, T_s, and T_c be the duration of the empty time slot, the average time the channel is busy due to a successful transmission, and the average time the channel is busy because of collisions, respectively. The average length of a slot time can be obtained by using the probability that the slot time is empty (i.e., $1-P_{tr,a}$), the probability that the successful transmission occurs (i.e., $P_{tr,a}P_{s,a}$), and the probability that the collision occurs (i.e., $P_{tr,a}(1-P_{s,a})$). Note that T_s and T_c are given as in Eqs. (27) and (28):

$$T_s = T_H + T_L + t_{ack} + T_{ACK} + 2IFS \tag{27}$$

Table 1
Parameters used in the numerical results.

Parameter	Value	Parameter	Value
Physical mode	PHY II	Degree of FOV	60°, 90°, 120°
CCA	Mode 3	Communication range	5 m
Modulation	OOK	Service area	20×20 m^2
Optical clock rate	120 MHz	Number of devices	2–40
Data rate	76.8 Mbps	Packet size	1024 bytes
Time of single optical clock	0.008 μs	PHY header	200 bits
Beacon order (BO)	10	MAC header	72 bits
Superframe order (SO)	10	ACK size	111 bits
aBaseSlot duration	60 optical clock	SIFS	12 optical clock
aBaseSuperframeDuration	960 optical clock	LIFS	40 optical clock
aTurnaroundTime	8 optical clock	macMaxFrameRetries	6

$$T_c = T_H + T_L + IFS, \tag{28}$$

where T_H, T_L, t_{ack}, T_{ACK}, and IFS refer to the time to transmit the header, the time to transmit the payload, the time to wait for the acknowledgement (ACK), the time to transmit the ACK, and the time of interframe space (IFS), respectively. Hence, S_a is obtained as in Eq. (29),

$$S_a = \frac{P_{tr,a}P_{s,a}L}{(1-P_{tr,a})\sigma + P_{tr,a}P_{s,a}T_s + P_{tr,a}(1-P_{s,a})T_c}. \tag{29}$$

Here, using S_a, we can derive S_{total}, which is the aggregate throughput referring to the summation of the normalized throughput for entire groups within the VPAN. S_{total} is obtained as in Eq. (30),

$$S_{\text{total}} = \sum_{a=1}^{n_g} S_a = \sum_{a=1}^{n_g} \frac{P_{tr,a}P_{s,a}L}{(1-P_{tr,a})\sigma + P_{tr,a}P_{s,a}T_s + P_{tr,a}(1-P_{s,a})T_c}, \tag{30}$$

where n_g is the number of groups.

Here, we derive the average delay of group a, $E(D_a)$, which is defined as the time from packet generation to successful reception or drop in group a, and given as in Eq. (31) [25],

$$E(D_a) = E(X_a)E(\text{length of a slot time for group } a), \tag{31}$$

where $E(X_a)$ is the average number of slot times for successful transmission in group a, which is calculated by using the number of slot times the packet should wait in each backoff stage and the probability that the packet reaches the corresponding backoff stage. $E(X_a)$ is obtained as in Eq. (32),

$$E(X_a) = \sum_{i=0}^{m} \left\{ \frac{W_i+3}{2} (p_I p_C + 1 - p_I)^i \right\}. \tag{32}$$

Thus, $E(D_a)$ is represented as in Eq. (33),

$$E(D_a) = \sum_{i=0}^{m} \left\{ \frac{W_i+3}{2} (p_I p_C + 1 - p_I)^i \right\} \{(1-P_{tr,a})\sigma + P_{tr,a}P_{s,a}T_s + P_{tr,a}(1-P_{s,a})T_c\}. \tag{33}$$

Finally, we can obtain the average delay for entire groups, $E(D)$, as in Eq. (34),

$$\begin{aligned} E(D) &= \frac{1}{n_g}\sum_{a=1}^{n_g} E(D_a) = \frac{1}{n_g}\sum_{a=1}^{n_g} \{E(X_a)E(\text{length of a slot time for group } a)\} \\ &= \frac{1}{n_g}\sum_{a=1}^{n_g} \left[\sum_{i=0}^{m} \left\{ \frac{W_i+3}{2} (p_I p_C + 1 - p_I)^i \right\} \{(1-P_{tr,a})\sigma + P_{tr,a}P_{s,a}T_s + P_{tr,a}(1-P_{s,a})T_c\} \right]. \end{aligned} \tag{34}$$

6. Numerical results

In this section, we present analytical results, through which the performance of GCT scheme is evaluated in terms of throughput and delay, and compared with that of IEEE 802.15.7 standard. We consider the various experimental scenarios with varying number of devices, number of classes, and degree of FOV. More specifically, the number of devices varies from 2 to 40, the numbers of classes are set to 2 and 3, and the degrees of FOV are set to 60°, 90°, and 120°. In our work, the spatial efficiency means higher throughput performance in a limited space. In this regard, we assume that the devices are randomly deployed in the fixed area of 20×20 m^2 and continuously attempt to transmit the packet of 1024 bytes in size

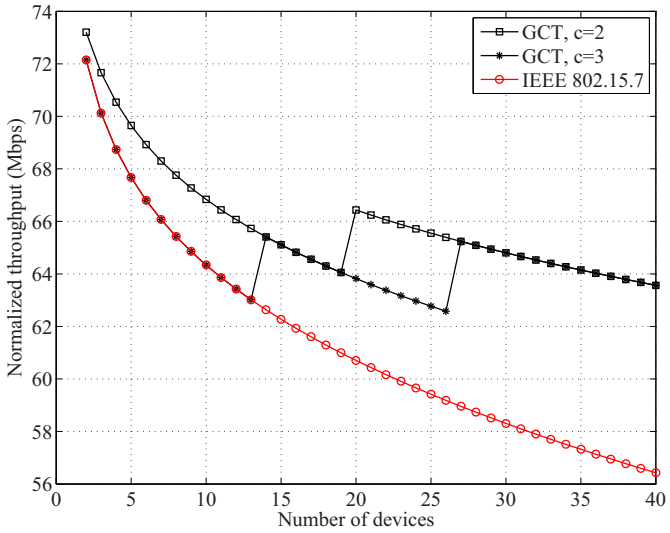

Fig. 4. Normalized throughput for a group.

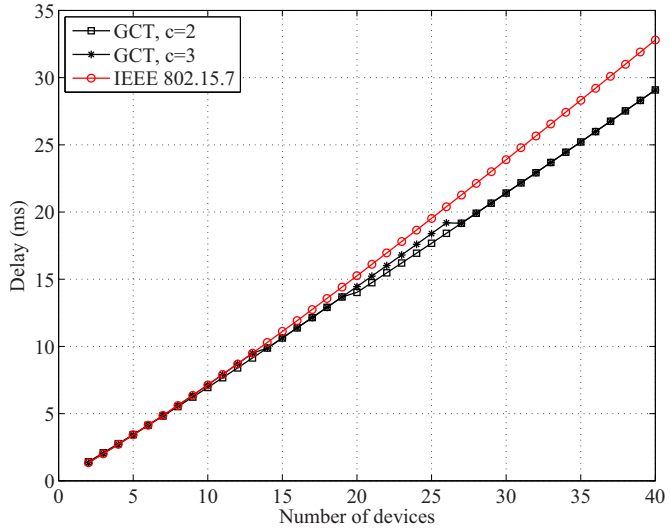

Fig. 5. Average delay for a group.

at a data rate of 76.8 Mbps. Each device is assumed to use the LED as a transmitter with 5-m communication range. For simplicity of analysis, we further assume that the devices always operate in active mode, for which the beacon order (BO) and the superframe order (SO) are set to the same value of 10, so that the devices do not enter the sleep mode. Note that these parameters (i.e., BO and SO) determine the beacon interval (i.e., length of superframe) and the superframe duration (i.e., active portion within superframe), respectively. The detailed set of parameters is listed in Table 1.

Fig. 4 compares the normalized throughputs for a group. In order to investigate the effect of BE decision by device grouping, we examined the change of normalized throughput performance with increasing number of devices in a single group. In the GCT, the reference value of the total number of devices is set to 40, and as the number of devices in the group changes from 2 to 40, the value of BE is differentiated into two levels when $c = 2$ and three levels when $c = 3$, respectively. In the case of IEEE 802.15.7, the total number of devices changes from 2 to 40, since there is no group setting. The throughput of the GCT decreases and then increases again at certain parts, which are the points that the number of devices in a group are 19 (in the case of $c = 2$), 13 and 26 (in the case of $c = 3$), respectively. This is because the GCT classifies the groups into c classes and assigns a different BE value to each group considering its class. On the other hand, the normalized throughput of the IEEE 802.15.7 standard continuously decreases as the number of devices increases. The IEEE 802.15.7 uses the fixed BE value (i.e., BE = 3) regardless of the number of devices. Thus, in the IEEE 802.15.7, the increase of device density causes frequent collisions, resulting in long channel access delays. However, the device grouping of GCT and the BE decision using

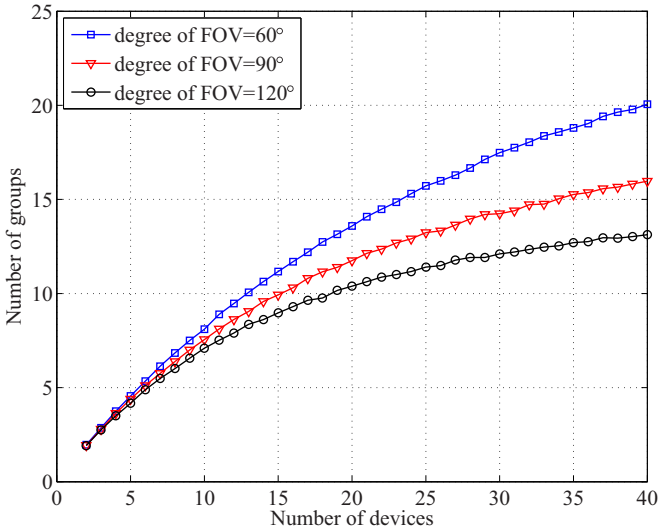

Fig. 6. Relationship between the number of groups and the degree of FOV.

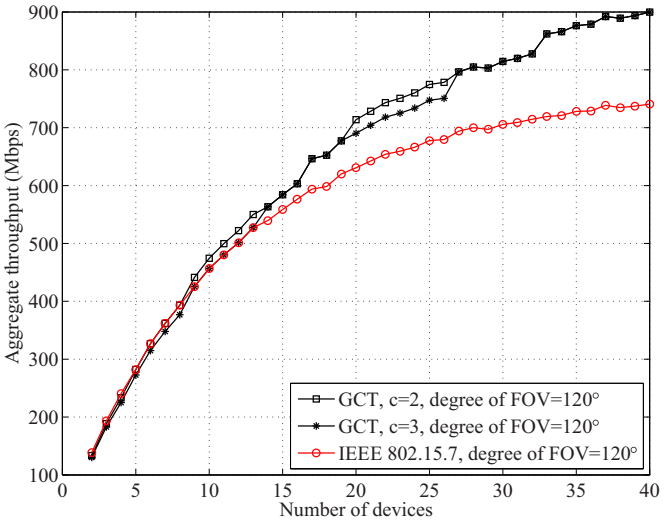

Fig. 7. Aggregate throughput for entire groups.

it mitigate the influence of the increase of the device density, thereby preventing unnecessary channel access delay and collision.

Fig. 5 shows an average delay for a group. We evaluated the average delay under the same conditions as Fig. 4. As a whole, the average delay increases as the number of devices increases, since the increase of device density causes long channel access delay due to the interference between the devices and the collisions. However, as with the results of Fig. 4, in the GCT scheme, its rate of increase temporarily decreases at certain parts and then returns again, which are the points that the number of devices in a group are 19 (in the case of $c=2$), 13 and 26 (in the case of $c=3$), respectively. Quantitatively, the GCT has 8.4% lower average delay than the IEEE 802.15.7 standard.

Here, to evaluate the aggregate throughput and the average delay for entire groups, we investigated the relationship between the number of groups and the degree of FOVs. Note that both the performance metrics are closely related to the number of created groups. To this end, we conducted an experimental simulation where we used three different degrees of FOV (i.e., 60°, 90°, and 120°). The simulation is iterated 1000 times for accuracy. As shown in Fig. 6, the number of groups decreases as the degree of the FOV increases. This is because an increase in the degree of FOV increases interference between the devices. More specifically, when the degree of FOV is 120°, 13.1% and 24.2% smaller numbers of groups are created compared with the 60° and 90° cases, respectively.

Figs. 7 and 8 show the aggregate throughput and the average delay for entire groups for various numbers of devices and numbers of classes (i.e., $c=2$ and $c=3$), where, we used 120° degree of FOV. The aggregate throughput increases as

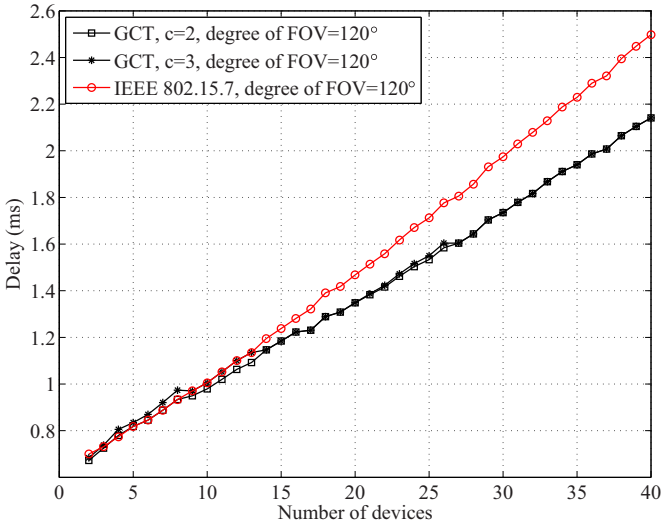

Fig. 8. Average delay for entire groups.

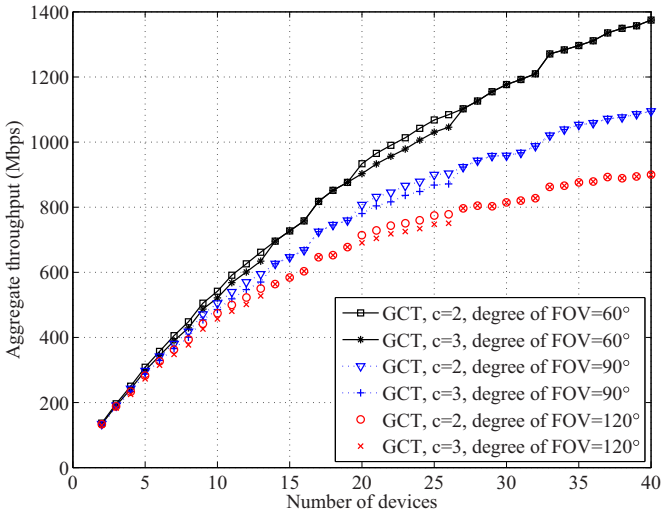

Fig. 9. Aggregate throughput for various degrees of FOV.

the number of devices increases. In Fig. 7, the GCT obtains higher aggregate throughput performance than the IEEE 802.15.7 standard because it can reduce the backoff delay and collisions by assigning the different BE values in accordance with the number of devices within a group. On average, the GCT obtains 12.5% and 11.0% higher aggregate throughput than the IEEE 802.15.7 when $c = 2$ and $c = 3$, respectively. Their difference in the aggregate throughput performance becomes greater as the number of devices increases, and as the number of classes increases. Note that this improvement shows the spatial efficiency of the GCT scheme.

Fig. 8 shows the average delay for entire groups for various numbers of devices. As shown in the figure, the average delay for entire groups is shorter than that of a single group case (i.e., Fig. 5). Considering the entire groups, as the number of devices increases, the devices are distributed into multiple groups. Thus, each group maintains fewer devices than a single group case. As a result, the delay due to interference and collision with neighboring devices is reduced. Note that, when $c = 3$ and the number of devices is between 3 and 8, the GCT shows a slightly longer delay that the IEEE 802.15.7. This is because, even if the number of devices increases, the GCT keeps a small value BE (i.e., BE = 2) in the corresponding interval, which is smaller than the default value of BE (i.e., BE = 3) of the IEEE 802.15.7 standard.

Fig. 9 compares the aggregate throughputs for various degrees of FOV. As can be seen from the results of Fig. 6, if the device uses a small degree of FOV, a larger number of groups are created. As the number of groups increases, more concurrent transmissions within the limited area become possible, resulting in increased aggregate throughput. Moreover,

when the device uses the same degree of FOV, the increase of the number of classes allows the fine adaptation of BE values. Therefore, the aggregate throughput performance of GCT scheme increases.

7. Conclusion

This paper presents the GCT scheme, which aims to improve the spatial efficiency of the IEEE 802.15.7-based VPANs. The operation of GCT consists of VLC device grouping and concurrent transmission scheduling. Through these operations, the GCT builds device groups considering the interference between the neighbors, and then allocates the different BE value to each group in accordance with the number of devices belonging to the group, thereby enabling the concurrent transmissions of adjacent neighboring device pairs. To evaluate the performance of GCT, we developed the analytical model using the discrete-time Markov chain. The numerical results show that the GCT achieves higher network performance in terms of normalized throughput, aggregate throughput, and average delay compared with the IEEE 802.15.7 standard.

Acknowledgments

This research was supported in part by the Leading Human Resource Training Program of Regional Neo Industry through the National Research Foundation of Korea (NRF) funded by the Ministry of Science, ICT and Future Planning (2016H1D5A1910427), by Basic Science Research Program through the NRF funded by the Ministry of Education (NRF-2017R1D1A1B03031055), and by NRF Grant funded by the Korean Government (NRF-2016-Fostering Core Leaders of the Future Basic Science Program/Global Ph.D. Fellowship Program) (2016H1A2A1908620).

References

[1] S. Rajagopal, R.D. Roberts, S.-K. Lim, IEEE 802.15.7 visible light communication: modulation schemes and dimming support, IEEE Commun. Mag. 50 (2012) 72–82.
[2] X. Bao, G. Yu, J. Dai, X. Zhu, Li-Fi: light fidelity-a survey, Wirel. Netw. 21 (2015) 1879–1889.
[3] S. Nobar, K.A. Mehr, J.M. Niya, Comprehensive performance analysis of IEEE 802.15.7 CSMA/CA mechanism for saturated traffic, IEEE/OSA J. Opt. Commun. Netw. 7 (2015) 62–73.
[4] H. Haas, L. Yin, Y. Wang, C. Chen, What is LiFi? J. Lightwave Technol. 34 (2016) 1533–1544.
[5] H. Burchardt, N. Serafimovski, D. Tsonev, S. Videv, H. Haas, VLC: beyond point-to-point communication, IEEE Commun. Mag. 52 (2014) 98–105.
[6] T. Komine, M. Nakagawa, Fundamental analysis for visible-light communication system using LED lights, IEEE Trans. Consum. Electron. 50 (2004) 100–107.
[7] IEEE Standard for Local and Metropolitan Area Networks–Part 15.7: Short-Range Wireless Optical Communication Using Visible Light, IEEE Standard (2011) 1–309.
[8] S. Dimitrov, H. Haas, Principles of LED Light Communications Towards Networked Li-Fi, first ed., Cambridge University Press, Cambridge, 2015.
[9] O. Ergul, E. Dinc, O.B. Akan, Communicate to illuminate: State-of-the-art and research challenges for visible light communications, Phys. Commun. 17 (2015) 72–85.
[10] P.H. Pathak, X. Feng, P. Hu, P. Mohapatra, Visible light communication, networking, and sensing: a survey, potential and challenges, IEEE Commun. Surv. Tutor. 4 (2015) 2047–2077.
[11] P.F. Mmbaga, J. Thompson, H. Haas, Performance analysis of indoor diffuse VLC MIMO channels using angular diversity detectors, J. Lightwave Technol. 34 (2016) 1254–1266.
[12] Y. Hong, J. Chen, Z. Wang, C. Yu, Performance of a precoding MIMO system for decentralized multiuser indoor visible light communications, IEEE Photon. J. 5 (2013).
[13] E.-J. Kim, S. Youm, C.-H. Kang, Power-controlled topology optimization and channel assignment for hybrid MAC in wireless sensor networks, IEICE Trans. Commun. E94-B (2011) 2461–2472.
[14] Z. Wang, Y. Liu, Y. Lin, S. Huang, Full-duplex MAC protocol based on adaptive contention window for visible light communication, J. Opt. Commun. Netw. 7 (2015) 164–171.
[15] C. Chen, S. Videv, D. Tsonev, H. Haas, Fractional frequency reuse in DCO-OFDM-based optical attocell networks, J. Lightwave Technol. 33 (2015) 3986–4000.
[16] Y. Wang, H. Haas, Dynamic load balancing with handover in hybrid Li-Fi and Wi-Fi networks, J. Lightwave Technol. 33 (2015) 4671–4682.
[17] E.-J. Kim, M. Kim, S.-K. Youm, S. Choi, C.-H. Kang, Priority-based service differentiation scheme for IEEE 802.15.4 sensor networks, Int. J. Electron. Commun. 61 (2007) 69–81.
[18] J.-H. Lee, I. Moon, Modeling and optimization of energy efficient routing in wireless sensor networks, Appl. Math. Model. 38 (2014) 2280–2289.
[19] M. Kim, C.-H. Kang, Priority-based service-differentiation scheme for IEEE 802.15. 4 sensor networks in nonsaturation environments, IEEE Trans. Veh. Technol. 59 (2010) 3524–3535.
[20] G. Bianchi, Performance analysis of the IEEE 802.11 distributed coordination function, IEEE J. Sel. Area Commun. 18 (2000) 535–547.
[21] H. Liu, L. Zhang, M. Jiang, Energy efficient medium access scheme for visible light communication system based on IEEE 802.15. 7 with unsaturated traffic, IET Commun. 10 (2016) 2534–2542.
[22] J.-H. Kwon, E.-J. Kim, Asymmetric directional multicast for capillary machine-to-machine using mm Wave communications, Sensors Basel 16 (2016) 151:1–151:17.
[23] L.X. Cai, L. Cai, X. Shen, J.W. Mark, REX: A randomized exclusive region based scheduling scheme for mm wave WPANs with directional antenna, IEEE Trans. Wirel. Commun. 9 (2010) 113–121.
[24] Z.N. Kong, D.H. Tsang, B. Bensaou, D. Gao, Performance analysis of IEEE 802.11e contention-based channel access, IEEE J. Sel. Area Commun. 22 (2004) 2095–2106.
[25] P. Chatzimisios, A.C. Boucouvalas, V. Vitsas, Packet delay analysis of IEEE 802.11 MAC protocol, Electron. Lett. 39 (2003) 1358–1359.